

# Circuit Model Equivalent for Load-Based Discharge of Supercapacitor Module

Aditya S Sengupta<sup>a</sup>, Nikhat Anjum<sup>b</sup>, Bidyut K Bhattacharyya<sup>c</sup>, Mukesh Kumar Ojha<sup>d</sup>, Shaik Qadeer<sup>e</sup> & Vijay Nath<sup>b\*</sup>

<sup>a</sup>Department of Electrical and Electronics Engineering, FST, ICFAI University Tripura, Kamalghat 799 210, India

<sup>b</sup>Department of Electronics and Communication Engineering, Birla Institute of Technology, Mesra 835 215, India

<sup>c</sup>Department of Electronics and Communication Engineering, National Institute of Technology, Agartala 799 046, India

<sup>d</sup>Department of Electronics and Communication Engineering, Institute of Technology, Greater Noida 201 310, India

<sup>e</sup>Department of Electrical Engineering, Muffakham Jah College of Engineering and Technology, Hyderabad 500 034, India

*Received: 9<sup>th</sup> June 2025; accepted: 16<sup>th</sup> December 2025*

The discharge behaviour of the Supercapacitor module (SCM) when it supplies a certain load is simulated. In scenario 1, a constant power application is powered by the SCM via a buck circuit, resulting in a constant output voltage. The voltage of the SCM will decay depending on the power drawn by the application and the different components of the circuit. The constant output voltage is obtained from the buck circuit by using a control circuit that will change the duty ratio as a function of the SCM voltage. The output remains unaffected by current changes from 450 mA to 1.2 A. The decay characteristics of SCM, including duty ratio and output voltage, are recorded. In scenario 2, another buck topology is designed that generates a decaying voltage from a power supply, almost like the voltage of the SCM. This circuit is used to power the same DC application via a DC-DC converter, and the respective decaying voltage, output voltage, and other parameters have been recorded. The simulation results from both scenarios have been tallied, leading to the inference that the circuit in scenario 2 can be used as an alternative to SCM for DC applications, and the successful operation time, a probable characteristic of SCM, can be estimated.

**Keywords:** Supercapacitor, Module, Discharge, Converter, Model

## 1 Introduction

Renewable energy has gained considerable momentum in recent years<sup>1-2</sup>. The use of supercapacitors in the field of renewable energy has become extensive, to the extent that supercapacitor technology is also utilised in renewable-based electric vehicle applications<sup>3-5</sup>. Even rural applications are catering to the use of renewable energy systems for storing energy generated from renewable sources. Different energy storage systems like double-layered capacitors, batteries, and fuel cells are used, and these energy storage systems play an important role in this field<sup>6-11</sup>. As the use of supercapacitors has become widespread, they have recently become a preferred choice for energy storage in the field of energy<sup>12</sup>.

Supercapacitors, often referred to as electrochemical double-layer capacitors (EDLC), were invented by scientists and patented in 1957 for use in recent technologies<sup>13-14</sup>. This supercapacitor technology is advantageous due to its short charging time, which has led to an increase in the number of applications associated with this technology<sup>15-16</sup>. Supercapacitor

technology, to some extent, outperforms other existing technologies, such as battery technology. Therefore, several battery-powered applications are integrating supercapacitors into their designs<sup>17-18</sup>. Supercapacitors have a very high-power density, allowing them to supply the instantaneous power required for sudden changes in current, thereby facilitating the simultaneous balancing of fast-changing power surges<sup>19-20</sup>. Most high-capacity supercapacitors available on the market have a very low terminal voltage. Therefore, a supercapacitor module, achieved by connecting a series-parallel combination of supercapacitors, is required for applications that require higher voltage and higher capacitance. Mega Farad Supercapacitors have also been designed to compensate for the high capacitance requirement<sup>21</sup>. It is quite evident from a prior article that charging supercapacitors is an efficient process and can increase the lifetime of applications<sup>22</sup>. Combined with its fast-charging capabilities, it supersedes other energy storage technologies in terms of powering different applications. The voltage from the SCM decays over time. Therefore, the power from supercapacitors is delivered via a DC-DC converter<sup>23-24</sup>.

\*Corresponding author: E-mail: vijaynath@bitmesra.ac.in











**5 Experimental Results**

The components used in the experiment are MOSFET IRF540N, op-amp LT1360CN8, Schottky diode 1N5819, and Zener diode 1N4732A. ‘V<sub>SCM</sub>’ was measured to be 11.34 V, ‘V<sub>i</sub>’ was taken as 12 V and ‘C<sub>SCM</sub>=850 F’, ‘C<sub>2</sub>=4700 μF’ and ‘R<sub>2</sub>’ is a series combination of 2 MΩ, two 400 KΩ, one 27 KΩ, one 10 KΩ and 1KΩ.

**5.1 Experimental Results for Figure 1**

From Fig. 8, the black solid line is the voltage of SCM with respect to time and is measured at node ‘A’ of Fig. 1. The dashed line is the respective output voltage of the converter measured at node ‘F’ of Fig. 1. The output voltage will fall to zero after approximately 156 minutes, as the peak voltage of the sawtooth wave will fall below the reference voltage of the PWM, as observed in Fig. 9.

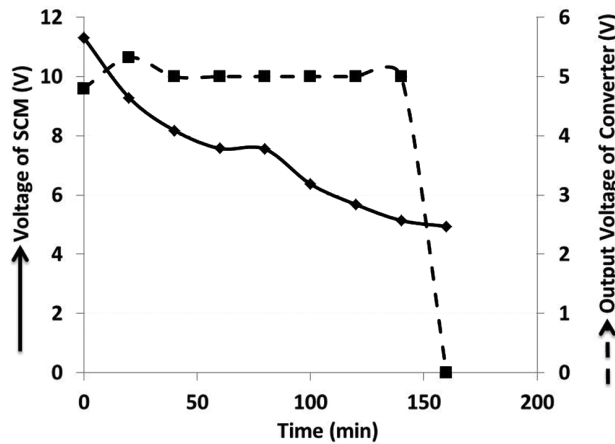


Fig. 8 — Input voltage of SCM and Output Voltage of the converter

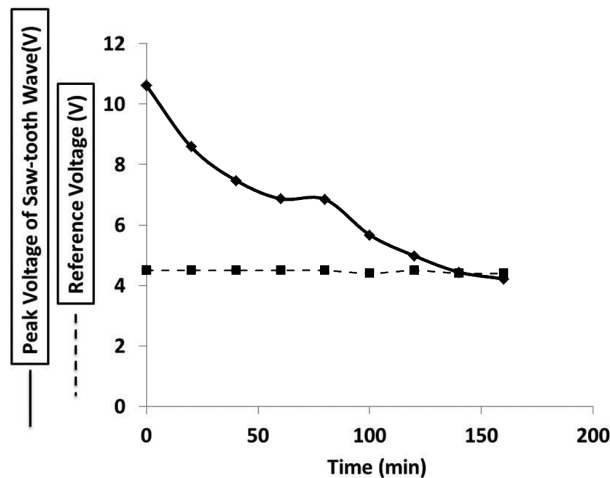


Fig. 9 — Input voltage of SCM and Output Voltage of converter

From Fig. 9, the black solid line curve is the peak value of sawtooth wave for PWM measured at node ‘C’ of Fig. 1. The black dashed line is the reference voltage of PWM and is measured at node ‘D’ of Fig. 1.

**5.2 Experimental Results for Figure 2**

From Fig. 10, the black solid line is a voltage profile similar to the voltage of SCM (modelled voltage of SCM) and is generated using the portion of the circuit in Fig. 2 bordered by dashed lines. This voltage profile is measured at node ‘A’ of Fig. 2. The black dashed curve in Fig. 10 is the output voltage of the converter when powered by the modelled SCM voltage profile and is measured at node ‘F’ of Fig. 2.

In Fig. 11, the black dashed curve represents the reference voltage of the PWM converter used to produce a voltage profile like that of a discharging

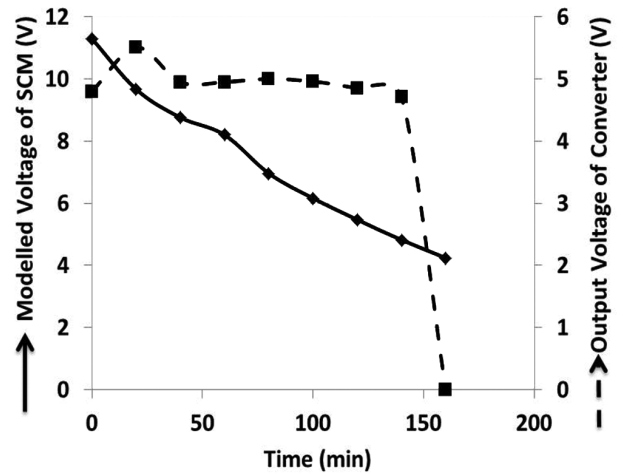


Fig. 10 — Modelled SCM voltage and Output Voltage of the converter

Fig. 11 — Reference Voltage and Peak Voltage of Sawtooth Wave for generating modelled SCM voltage

SCM. This voltage is the voltage of Capacitor  $C_2$  pre-charged to 5V and now discharging under the influence of  $R_2$ . This voltage is measured across  $C_2$ . The black solid line represents the peak voltage of a constant sawtooth wave at 5V. These two waveforms are compared by op-amp A3 to produce a PWM signal with a decreasing duty ratio.

## 6 Discussion

If ' $E_{SCM}$ ' is the energy supplied from SCM, ' $P_o$ ' power consumed by the application, ' $P_{diss}$ ' is the power dissipated in the ESRs of SCM and ' $P_{loss}$ ' is the other cumulative losses in the circuit are given, then the time ' $t$ ' for which the application would run can be found out using Eq. (3).

$$t = \frac{E_{SCM}}{P_o + P_{diss} + P_{loss}} \quad \dots (3)$$

$$V_{SCM-final} = V_{SCM-initial} e^{-t/\tau} \quad \dots (4)$$

$$\tau = R_2 C_2 \quad \dots (5)$$

$$L = \frac{V_o(1-D_{min})}{\Delta i_L f_s} \quad \dots (6)$$

$$C = \frac{\Delta i_L}{8(\Delta V_o) f_s} \quad \dots (7)$$

This time ' $t$ ' is also the time needed by the SCM voltage to decay from its initial value ' $V_{SCM-initial}$ ' to its final value ' $V_{SCM-final}$ '. The time constant ' $\tau$ ' of this voltage decay can be calculated from Eq. (2). After this, the values of  $R_2$  and  $C_2$  are not supposed to be calculated but rather chosen such that Eq. (5) is satisfied, as the product of  $R_2$  and  $C_2$  is the time constant ' $\tau$ ' for the voltage decay of SCM. Now, these  $R_2$  and  $C_2$  may be used in the portion of the circuit in Fig. 2, inside the black dashed border, to model the discharge behaviour of SCM. For the calculation of other parameters frequency of the switching pulse ' $f_s$ ' provided to the MOSFET of the buck converter should be known. The other parameters, like inductance value, should be calculated using Eq. (4), and the capacitance value must be chosen to be a value higher than calculated using Eq. (6) as per the reference given <sup>43-44</sup>. The value of ' $\Delta i_L$ ' Eq. (7) should be taken to be 10 % of the output current, and ' $\Delta V_o$ ' is the amount of ripple to be allowed in the output. ' $D_{min}$ ' is the duty ratio corresponding to the highest input voltage for constant output voltage and the

lowest output voltage for constant input voltage. This methodology for calculating the operation time of any application running on an SCM is applicable to any SCM of any rating and can also be used to model the discharge characteristic of an SCM.

### 6.1 Analysis

The model for implementing a DC-DC converter-based circuit that generates the behavior of a discharging supercapacitor has been simulated and verified experimentally. This model does not incorporate temperature dependencies, primarily because it is an RC-based circuit; however, it can be concluded that SCM will discharge at a comparatively faster rate at higher temperatures (45-46). The current model does not deal with the ageing effect on SCM. But it is evident from<sup>47</sup> that ageing of SCM would decrease its effective capacitance to some extent, and the equivalent series resistance (ESR) of SCM should increase linearly. The discharge characteristics are not linear but rather exponential, as evident from both the simulation and experimental results. Thus, nonlinearities are already part of the SCM discharge characteristics. Although the actual discharge characteristics and the modelled characteristic are similar but not exact, to better understand the characteristics, the absolute percentage deviation between the values of voltage of the original supercapacitor characteristic and that modelled using dc-dc converter at different time instants has been graphically shown below:

From Fig. 12, it can be seen that the absolute percentage deviation in values of actual SCM voltage

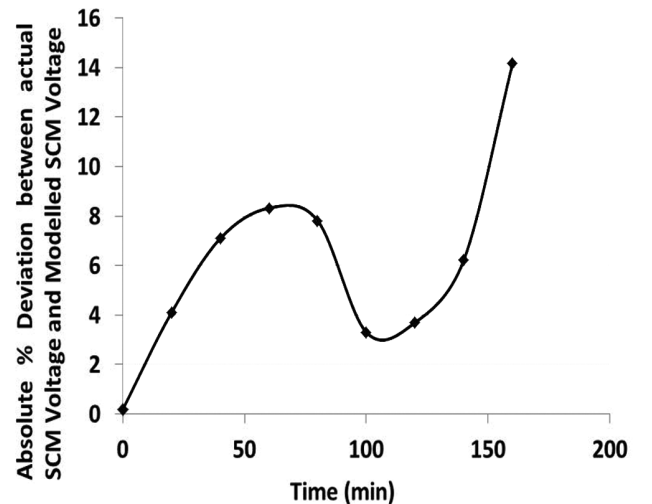


Fig. 12 — Absolute percentage deviation between actual SCM voltage and modeled SCM voltage

Table 1 — Comparative Analysis

Reference Number	Operating Voltage (V)	Capacitance (F)	Power Dissipation Element	Model Build	Load Condition
[36]	2.7	100	8.1 m $\Omega$ and 8.7 m $\Omega$	RC based transmission line model	Resistive load
[37]	2.5	110	0.0100478 and 17.4976	two Branch model	no load
	2.5	200	0.0088521 and 8.767		
	2.5	350	0.0048032 $\Omega$ and 5.55652 $\Omega$		
	2.7	600	0.002848 $\Omega$ and 3.09927 $\Omega$		
[38]	2.7	650	098 m $\Omega$ , 2.54 $\Omega$ and 43.79 $\Omega$ ,	Three branch RC model	no load
[39]	2.7	2600	0.5 m $\Omega$	Simulation model	no load
[41]	2.7	3000	290 $\mu\Omega$	RC model	simple resistive
This Work	11.6	850	0.23 m $\Omega$	Power Electronic model	Constant Power Draw

and modeled SCM voltage ranges between 0.18 % and 14.17 %.

A comparative study can be conducted based on several parameters, such as the basic concept of the work and the methodologies used. In this article, a comparative study is conducted based on the specifications of the supercapacitor used, the type of circuit equivalent, the power dissipation element, and the application type, among others. Only ESR is considered for the power dissipation element. In this work, the SCM is a series combination of four identical supercapacitors, each with a 2.9 V voltage and a 3400 F capacitance, and an ESR of 0.23 m $\Omega$ . The total power dissipation amounts to approximately 0.15 mW. The different parameters based on which comparisons have been made are listed in Table 1. In only one supercapacitor cell, having a capacitance of 100 F and a voltage of 2.7 V, is modelled using an RC-based transmission line model and using a characterization setup, different characteristics of the supercapacitor are found out, and those characteristics are put in a MATLAB Simulink model to get a finalized equivalent model<sup>36</sup>. This is entirely different from the work demonstrated here, in which SCM is used by connecting supercapacitor cells in series. After running a constant power application from this SCM via a buck circuit, the discharge characteristic is determined and eventually modelled using another buck circuit. In the two-branch model, supercapacitors of different specifications are tested, and the values of their power loss elements are determined; however, the equivalent circuit is not used to supply a constant power load<sup>37-38</sup>. An equivalent circuit model for a supercapacitor with a 2.7 V and 650 F rating was developed. The power loss

element values in this model were also determined; however, this equivalent model for a supercapacitor has not been used to supply any constant power-drawing load. An RC-based transmission line model for a 2.7 V, 2600 F supercapacitor is designed, and its various parameters are determined for self-discharge analysis. The model is verified using MATLAB and LabVIEW; however, the circuit equivalent has not been verified for load-dependent discharge of supercapacitor<sup>39</sup>. In an RC-based circuit equivalent, a supercapacitor of 2.7 V, 3000 F is modelled, and the equivalent model is shown to be valid only for a resistive load. Based on this, the power loss elements of the equivalent model have been calculated. All the above-described works have no similarity to the work given in this article.

## 7 Conclusion

For recreating the discharge profile of SCM using a power electronic circuit under different constant power applications as load, an SCM of 850 F and nearly 11.6 to 11.34 V is used to supply a constant power drawing application via a power electronic converter, and the voltage decay characteristic of SCM is recorded in Fig. 3 along with the output voltage of the converter circuit which is given in Fig. 5. Thereafter, the operation time, as determined from the simulation results in Fig. 2, and the time constant of voltage decay are estimated mathematically using Eqs. (1) and (2). Then, a combination of resistance and capacitance values is chosen for the time constant, and this combination is used in the PWM switching circuit of another buck topology, which uses the battery as input, as shown in Fig. 2. This Buck topology is used in place of the SCM

as the source to power the entire circuit of Fig. 1. The SCM voltage decay modelled by the circuit equivalent of SCM (shown by the portion of the circuit in Fig. 2 bordered by black dashed lines) is recorded in Fig. 6. It has been found to closely match the actual voltage decay characteristic of SCM, as shown in Fig. 3. The output voltage of the circuit in Fig. 1 (Given by a black line in Fig. 5) is found to be almost identical to the output voltage of the circuit given in Fig. 2 (given by a black line in Fig. 7). Also, the operating time is almost 2 hours and 45 minutes. Hence, it can be concluded that the circuit equivalent of SCM can be used as a test circuit in place of the SCM to supply a constant power application, and the different parameters, like circuit operation time, etc., can be accurately estimated, especially because the output voltages of both circuits in Figs. 1-2 are found to be almost identical. The experimental results further validate the model, as the output voltage of the converter is almost identical (Figs. 8 and 10) for both cases: when the converter is powered from the SCM and when it is powered from the modelled voltage of the SCM. Although there is a deviation in the actual voltage profile of SCM (Fig. 8) and the one modelled using a DC-DC converter (Fig. 10), the absolute % deviation in values is quite small, with the highest being approximately 14.17 %.

## References

- 1 Reddy T S, Junaid K A, Sukhi Y, Jeyashree Y, Kavitha P & Nath V, *Adv Electr Eng Electron Energy*, 5 (2023) 100206.
- 2 Junaid K A, Sukhi Y, Anjum N, Jeyashree Y, Ahamed A F, Nath V, Debbarma S, *et al.*, *Adv Electr Eng Electron Energy*, 5 (2023) 100271.
- 3 Wang S, Wei T & Qi Z, *Proceed ISES World Congress 2007 Springer Berlin Heidelberg*, 1 (5) (2008) 2805.
- 4 Kinjo T, Senjyu T, Urasaki N & Fujita H, *IEEE Trans Energy Convers*, 21 (2006) 221.
- 5 Zhang Z, Zhang X, Chen W, Rasim Y, Salman W, Pan H & Wang C, *Appl Energy*, 178 (2016) 177.
- 6 Bhatia C M, Banga S, Khurana M, Malhotra S, Juneja B, Bhardwaj H & Kapahi M, *IETE Tech Rev*, 23 (2006) 321.
- 7 Hasanpour S, Baghrmian A & Mojallali H, *IEEE Trans Power Electron*, 35 (2020) 8088.
- 8 Neto P B, Saavedra O R & De Souza Ribeiro L A, *IEEE Trans Sustain Energy*, 9 (2018) 1618.
- 9 Ganesan S, Subramaniam U, Ghodke A A, Elavarasan R M, Raju K & Bhaskar M S, *IEEE Access*, 8 (2020) 188861.
- 10 Hamajima T, Amata H, Iwasaki T, Atomura N, Tsuda M, Miyagi D & Kajiwara M, *IEEE Trans Appl Superconduct*, 22 (2012) 5701704.
- 11 Aneke M & Wang M, *Appl Energy*, 179 (2016) 350.
- 12 Malamaki K-N D, Casado-Machado F, Barragan-Villarejo M, Gross A M, Kryptonidis G C, Martinez-Ramos J L & Demoulias C S, *IEEE Trans Industry Appl*, 58 (2022) 7581.
- 13 Becker H I, *General Electric Co, USA*, (1957) 2800616.
- 14 Shylashree N, Amulya M S, Disha G R, Praveena N, Verma V K, Muthumanickam S & Nath V, *IETE J Res*, 1 (2023).
- 15 D Arnaudov N H, *19<sup>th</sup> International Symposium on Electrical Apparatus and Technologies (SIELA), Bourgas, Bulgaria*, 1 (2016).
- 16 Sengupta A S, Satpathy S, Mohanty S P, Baral D & Bhattacharyya B K, *IEEE Consumer Electron Mag*, 7 (2018) 50.
- 17 Rocabert J, Capó-Misut R, Muñoz-Aguilar R S, Candela J I & Rodríguez P, *IEEE Trans Industry Appl*, 55 (2019) 1853.
- 18 Roy P, He J & Liao Y, *IEEE Access*, 8 (2020) 210099.
- 19 Kollimalla S K, Mishra M K & Narasamma N L, *IEEE Trans Sustain Energy*, 5 (2014) 1137.
- 20 Camara M B, Gualous H, Gustin F, Berthon A & Dakyo B, *IEEE Trans Industrial Electron*, 57 (2010) 587.
- 21 Kazerani A O, *IEEE Trans Vehicular Technol*, (2015) 4449, doi: 10.1109/TVT.2014.2371912.
- 22 Simjee F I & Chou P H, *IEEE Trans Power Electron*, 23 (2008) 1526.
- 23 Sengupta A S, Chakraborty A K & Bhattacharyya B K, *IETE J Res*, 66 (2018) 115.
- 24 Sengupta A S, Mohanty S P & Bhattacharyya B K, *IET Power Electron*, 11 (2018) 1946.
- 25 Padhee S, Pati U C & Mahapatra K, *IETE Tech Rev*, 35 (2016) 99.
- 26 Cornea O, Hulea D, Muntean N & Andreescu G-D, *IEEE Access*, 8 (2020) 136092.
- 27 H Antchev A A, *In Proceedings 17th Conference on Electrical Machines, Drives and Power Systems (ELMA), Sofia, Bulgaria*, (2021) 1, doi: 10.1109/ELMA52514.2021.9502967.
- 28 Zhou G, Xu J & Wang J, *IEEE Trans Industrial Electron*, 61 (2014) 1280.
- 29 Xu J & Qin M, *IET Power Electron*, 3 (2010) 391.
- 30 Chung J -E-M, *IEEE Electron Device Lett*, 44 (10) (2023) 1792.
- 31 R M Reddy M D, *IEEE Trans Circuits Syst II*, 70 (7) (2023) 2580.
- 32 Zubieta L & Bonert R, *IEEE Trans Industry Appl*, 36 (2000) 199.
- 33 Gualous H, Bouquain D, Berthon A & Kauffmann J M, *J Power Sources*, 123 (2003) 86.
- 34 Fletcher S, Black V J & Kirkpatrick I, *J Solid State Electrochem*, 18 (2013) 1377.
- 35 Umanand L, *Power Electron Essential Appl, Wiley India Pvt. Ltd, 1<sup>st</sup> Edn*, (2009).
- 36 Logerais P O, Camara M A, Riou O, Djellad A, Omeiri A, Delaleux F & Durastanti J F, *Int J Hydrogen Energy*, 40 (2015) 13725.
- 37 Faranda R, *Electric Power Syst Res*, 80 (2010) 363.
- 38 Liu K, Zhu C, Lu R & Chan C C, *IEEE Trans Plasma Sci*, 41 (2013) 1267.
- 39 Kim S-H, Choi W, Lee K-B, & Choi S, *IEEE Trans Power Electron*, 26 (2011) 3377.
- 40 Chai R, & Zhang Y, *IEEE Trans Power Electron*, 30 (2015) 6720.
- 41 Liu C, Wang Y, Chen Z & Ling Q, *J Power Sources*, 374 (2018) 121.
- 42 Pourkheirollah H, Keskinen J, Mäntysalo M & Lupo D, *IEEE Trans Power Electron*, 535 (2022) doi:10.1016/j.jpowsour.2022.231475.
- 43 Hauke B, *Texas Instr*, Application Report SLVA477B Rev, (2015).

- 44 Xiong G, Kundu A & Fisher T S, *Springer Briefs in Thermal Engineering and Applied Science*, DOI 10.1007/978-3-319-20242-6\_4
- 45 Köps L, Kreth F A, Klein M & Balducci A, *J Power Sources*, 581 (2023), doi.org/10.1016/j.jpowsour.2023.233480.
- 46 Sedlakova I V, Sikula J, Majzner J, Sedlak P, Kuparowitz T, Buegler B & Vasina P, *Metrol Measure Syst*, 23 (2016), DOI: 10.1515/mms-2016-0038.
- 47 Anjum N, Yadav V K S & Nath V, *IJMIT*, 1 (2) (2023) 82.
- 48 Suman P N, Kumari J, Anjum N, Kiran A, Muthumanickam S, Rai A, Debbarma S, Kumar S, Ojha M K, Nath V & Mishra G K, *IETE J Res*, (2024) 1, <https://doi.org/10.1080/03772063.2024.2307426>
- 49 Anjum N, Yadav V K S & Nath V, *Ind J Pure Appl Phys*, 63 (6) (2025) 517.
- 50 Sharma D & Nath V, *Circuits Syst Signal Process*, 44 (2025) 2266.
- 51 Reddy S T & Nath V, *Sci Rep*, 15 (2025) 9585.
- 52 Sharma D & Nath V, *Analog Integr Circ Sig Process*, 122 (2025) 39.